Zero-field magnetization reversal of two-body Stoner particles with dipolar interaction

Z. Z. Sun,[a] A. López,[b] and J. Schliemann
Institute for Theoretical Physics, University of Regensburg, D-93040 Regensburg, Germany

(Received 10 December 2010; accepted 13 March 2011; published online 16 May 2011)

We investigate magnetization reversal in a system of two Stoner particles with uniaxial anisotropies both subject to a static and antiparallel magnetic field, and taking into account their mutual dipolar interaction. We identify an interesting regime of stable synchronized magnetic dynamics where the two particles are implementing a single information bit. Here a modified Stoner-Wohlfarth limit occurs which results in a dramatically lower critical switching field H_c (including $H_c = 0$) and also a substantially shorter reversal time. Our analytical results are verified by numerical simulations and offer new technological perspectives regarding devices for information storage and/or fast magnetic response. © *2011 American Institute of Physics*. [doi:10.1063/1.3581106]

I. INTRODUCTION

Magnetization reversal in magnetic nanostructures has recently attracted explosive attention due to the fundamental interest of the traditional magnetism and the newly emerging spintronics community, but also, and in particular, because of the enormous potential applications in information industry, such as hard disk technology, magnetic memory, and logic devices.[1,2]

Recent technological advances[3–6] allow for the fabrication of smaller and smaller magnetic nanoparticles (often referred to as Stoner particles), in which all the atomic moments can rotate coherently under low thermal excitation due to the strong exchange interaction between them. This single-domain type magnetization dynamics under static or pulsing magnetic fields has been extensively studied, both theoretically and experimentally,[7–17] showing to be in good agreement. Current induced magnetization reversal phenomenon has also attracted much interest where a spin-polarized current flowing through magnetic multilayers or spin-valves can directly manipulate the magnetization,[18–21] which promises broad applications in future. From an industrial point of view, important issues include lowering the critical switching field (or current), and achieving shorter reversal times.

In a Stoner particle with uniaxial anisotropy, the magnetization reversal means that the system changes from one valley to another across the barrier in between on the system energy surface. The critical switching field H_c can be defined as the minimum external field to complete such a reversal path. The magnitude of H_c was first studied by Stoner and Wohlfarth[7] and they predicted that H_c equals the field just capable of eliminating the energy barrier, which is now called the well-known Stoner-Wohlfarth (SW) limit. Later numerical simulations and experiments[8–11] confirmed the correctness of the SW limit in the ringing-motion mode where magnetic field is parallel to the particle easy axis (EA), but also showed that H_c can be lower than the SW limit in the precessional-reversal mode where field is noncollinear (perpendicular) to EA. The physical reason of the lower H_c was well explained by that the system may run over the energy barrier by touching the saddle point, implying the barrier exists still at corresponding lower field.[16] H_c can also be lowered substantially by applying a time-dependent field or microwave radiation.[15–17] However, producing an optimized field pulse pattern is still a big challenge to current experimental techniques.

Moreover, since nanoparticles are fabricated in array patterns,[3–6] the dipole-dipole interaction (DDI) between them possesses an important role and will affect the magnetic switching behaviors. A system of two Stoner particles could be the simplest system to investigate the DDI effect. In fact a quite number of studies have already put on this subject.[22–28] Bertram *et al*. firstly predicted that there may coexist coherent rotation and fanning modes in two magnetic dipoles system.[22] Later Chen *et al*. have obtained analytical forms of energy barriers under a static consideration of the energy surface variation. The dipolar interaction can also assist the switching of one particle and influence its hysteresis loop in the two-body system, which was numerically showed in Ref. 26.

In this paper, we shall go further the previous studies and predict a new technological perspective in the two-body system both analytically and numerically: the critical switching field H_c on both particles can be dramatically lowered (even including $H_c = 0$, neglecting environmental fluctuations) by appropriately engineering the magnetic DDI (i.e., the distance) between the two Stoner particles. We identify a stable regime of synchronized magnetization dynamics in the two-body system, where it can be regarded, in the sense of information technology, as a single bit. We analytically obtain a modified SW limit for two typical geometrical configurations of the two dipoles. Moreover, DDI also contributes to substantially shorten the reversal time around the zero-field regime, as compared to the single particle case (without DDI). We illustrate the experimental feasibility of

[a]Electronic mail: phzzsun@gmail.com.
[b]Permanent address: Centro de Física, Instituto Venezolano de Investigaciones Científicas, Caracas 1020-A, Venezuela.

realizing the zero-field scheme on the example of cobalt nanoparticles. The paper is organized as follows: Sec. II describes the model and main dynamical equations, and Sec. III includes the main analytical and numerical results and a discussion. We close with conclusions.

II. MODEL DESCRIPTION

The magnetization dynamics of two Stoner particles system being subject to DDI and an external magnetic field is governed by the Landau-Lifshitz-Gilbert (LLG) equation,[16,29,30]

$$\dot{\vec{m}}_i = -\vec{m}_i \times \vec{h}_i' + \alpha \vec{m}_i \times \dot{\vec{m}}_i. \tag{1}$$

Here $\vec{m}_i = \vec{M}_i/M_s$ is the normalized magnetization vector of the ith particle, $(i = 1, 2)$. $M_s = |\vec{M}_i|$ is the saturation magnetization of either particle, and α is the Gilbert damping coefficient. For simplicity, we are assuming the two particles to be completely identical in shape, volume, α, and M_s. The unit of time is set to be $(|\gamma|M_s)^{-1}$, where γ is the gyromagnetic ratio, and the total effective field $\vec{h}_i'$ is given by $\vec{h}_i' = -\partial E/\partial \vec{m}_i$, where

$$E = -\sum_{i=1,2} (k m_{i,z}^2 + \vec{m}_i \cdot \vec{h}) + \eta[\vec{m}_1 \cdot \vec{m}_2 - 3(\vec{m}_1 \cdot \hat{n})(\vec{m}_2 \cdot \hat{n})] \tag{2}$$

is the total energy per particle volume V in units of $\mu_0 M_s^2$ (μ_0: vacuum permeability). Here both particles have their EAs along the z-direction, and the uniaxial parameter k summarizes both shape and exchange contributions to the magnetic anisotropy. In addition, $\vec{h} = \vec{H}/M_s$ where $\vec{H}$ is a homogeneous and static external field on both particles. The parameter $\eta \equiv \frac{V}{(4\pi d^3)}$ is a geometric factor characterizing the DDI with d being the fixed distance between the two particles whose direction is described by the unit vector $\hat{n}$. Here we omit the exchange interaction energy between the two particles since it becomes important only at very small particle distances. Moreover, in the synchronized magnetic dynamics to be investigated below, it only contributes a constant to the energy and will therefore not change the physical behavior.

Let us focus on two typical geometrical configurations where the connecting unit vector $\hat{n}$ is either perpendicular or parallel to the anisotropy axes, referred to as PERP and PARA configuration, respectively (see insets in Fig. 1). That is, introducing spherical coordinates $\vec{m}_i = (\sin\theta_i \cos\phi_i, \sin\theta_i \sin\phi_i, \cos\theta_i)$, $\hat{n} = (\sin\theta_n \cos\phi_n, \sin\theta_n \sin\phi_n, \cos\theta_n)$, we have $\theta_n = \pi/2$ for PERP configuration and $\theta_n = 0$ for PARA (or $\theta_n = \pi$ since DDI is invariant under $\hat{n} \mapsto -\hat{n}$). Moreover, without loss of generality, we can let $\phi_n = 0$ for both configurations, i.e. $\hat{n} = \hat{x}$ in PERP and $\hat{n} = \hat{z}$ in PARA, as shown in insets of Fig. 1. Furthermore, we concentrate on the synchronized magnetic dynamics of the two Stoner particles, where both magnetization vectors remain parallel throughout the motion, $\theta_1 = \theta_2 = \theta$, $\phi_1 = \phi_2 = \phi$. Thus, the two particles behave like a single entity, and this two-body Stoner particle can be regarded as a computer information bit. We have verified by numerical simulations (see discussion below) that this dynamical regime is stable against perturbations. For this synchronized motion mode, the nonlinear coupled LLG Eq. (1) read in spherical coordinates

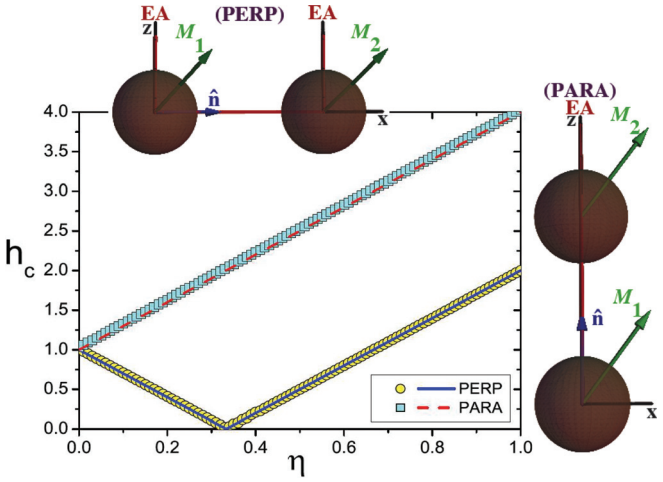

FIG. 1. (Color online) The (normalized) critical switching field h_c versus the DDI strength η for PERP and PARA configuration illustrated in the insets. Analytical results (solid and dashed lines) are compared with numerical findings (circles and squares). The system parameters are $k = 0.5$ and $\alpha = 0.1$.

$$\begin{aligned} \dot{\theta} + \alpha \sin\theta \dot{\phi} &= -3\eta \cos\psi \sin\theta_n \sin\phi, \\ \alpha\dot{\theta} - \sin\theta\dot{\phi} &= h\sin\theta - k\sin 2\theta + \frac{3\eta}{2}\frac{\partial \cos^2\psi}{\partial\theta}, \end{aligned} \tag{3}$$

where ψ is the angle between $\vec{m}$ and $\hat{n}$, i.e., $\cos\psi = \cos\theta\cos\theta_n + \sin\theta\sin\theta_n\cos\phi$. Here we have put $\vec{h} = -h\hat{z}$ (antiparallel) along the EA, which is the conventional field configuration for reversing a magnetic bit. The above equations are the starting point of our numerical calculations to be discussed below.

III. RESULTS AND DISCUSSION

A. Analytical results: Modified SW limit

In order to analytically explore the SW limit for magnetic reversal,[7,16] we assume the external field to lie in the plane spanned by the anisotropic axis and the interparticle direction, $\vec{h} = h_z\hat{z} + h_x\hat{x}$. The energy for the synchronized motion mode takes the form $E = -2k\cos^2\theta - 2h_z\cos\theta - 2h_x\sin\theta + \eta(1 - 3\cos^2\psi)$ with $\psi = \theta - \theta_n$. The SW limit occurs at the inflection of the energy as a function of θ, i.e., $\partial E/\partial\theta = \partial^2 E/\partial\theta^2 = 0$. An elementary calculation translates this condition into

$$\left(\frac{h_x}{2k \mp 3\eta}\right)^{2/3} + \left(\frac{h_z}{2k \mp 3\eta}\right)^{2/3} = 1, \tag{4}$$

where the minus (plus) sign corresponds to the PERP (PARA) configuration, respectively. Note that in the absence of DDI, $\eta = 0$, the above equation just recovers the usual SW limit for a single Stoner particle.[7,16] As a result, the critical switching field h_c (applied antiparallel to the EA) is given by

$$h_c^{\mathrm{PERP}} = |2k - 3\eta|, \quad h_c^{\mathrm{PARA}} = 2k + 3\eta. \tag{5}$$

This analytical solution (5) is shown by the solid and dashed lines in Fig. 1.

Moreover, the above findings imply the remarkable observation that in the PERP configuration there exists a critical DDI strength $\eta_c = 2k/3$ such that *the critical switching field vanishes!* ($h_c = 0$). Although this result was implied in some pioneering studies,[22,23] we would like to point out that the importance of zero-field synchronized switching may have a new technological prospective for nanomagnetism storage industry, which will be the focus of our paper and discussed in detail.

The zero-field condition is achieved for interparticle distances given by

$$d_c = \left(\frac{3\mu_0 M_s^2 V}{8\pi K}\right)^{1/3}, \tag{6}$$

where $K = k\mu_0 M_s^2$ is the standard anisotropy coefficient. Remarkably, the above condition is independent of the damping, and its physical contents can be illustrated in terms of the energy landscape. In the PERP configuration, the energy in the absence of an external field is $E = -2\eta + 3(\eta - \eta_c)\cos^2\theta$. Thus, for $\eta = \eta_c$, any angle θ represents an equilibrium position such that an arbitrary small field is sufficient to rotate the magnetization vector along the field direction, implying the possibility of zero-field reversal. Moreover, for $\eta > \eta_c$, the zero-field ground state in this synchronized motion mode is given by $\theta = \pi/2$, i.e., the synchronized magnetization vectors point along the interparticle axis, while for $\eta < \eta_c$, the ground state magnetization is along the EAs, $\theta = 0, \pi$.

B. Numerical Results

In order to complement and quantitatively support our previous discussion, we have performed numerical simulations of the dynamical LLG Eq. (3) using the fourth-order Runge-Kutta scheme. We consider a range of the DDI parameter of $0 \le \eta \le 1$. The case, $\eta = 0$ corresponds to the limit $d \to \infty$, i.e., the two nanoparticles being infinitely apart. Large η can be realized by fabricating magnetic nanoparticles of ellipsoidal shape allowing for a closer proximity. Throughout the numerical results shown here, we use a typical damping parameter of $\alpha = 0.1$. In Fig. 1 we compare simulation results for the critical switching field with the analytical formulae (5), both findings being in excellent agreement. The critical switching field in the PARA configuration is always higher than the value without DDI. Thus, only the PERP configuration will be useful for possible technological applications.

Let us now turn to the reversal time T_r, i.e., the duration of the reversal process of the magnetization direction changing the angle θ from 0 to π. To avoid the metastable points $\theta = 0, \pi$, we introduce two small deviations δ_i, δ_f, by defining $\theta_i = \delta_i$ (i.e., $m_z \approx 1$) and $\theta_f = \pi - \delta_f$ (i.e., $m_z \approx -1$), which leads to a finite reversal time in our simulations. In the PARA configuration, one can derive a closed analytical expression for this quantity (see Appendix),

$$T_r = -\lambda\left\{\frac{\ln\delta_i}{h-h_0} + \frac{\ln\delta_f}{h+h_0} + \frac{h_0\ln[(h+h_0)/(h-h_0)] - h\ln 4}{h^2 - h_0^2}\right\}, \tag{7}$$

where $h_0 = 2k + 3\eta$ and $\lambda = \alpha + \alpha^{-1}$. Note that the case $\eta = 0$ also includes the PERP configuration since both configurations are indistinguishable here and just for a single Stoner particle. The first two terms will dominate the major contributions in T_r since δ_i, δ_f is small.

In Fig. 2(a) we show simulation results for T_r in the PARA configuration, where we have set $k = 0.5$, $\delta_i = \delta_f = 0.001$, and various η. The simulation data is well described by the approximate expression $T_r \simeq \frac{[2\lambda h(-\ln\delta_i)]}{(h^2 - h_0^2)}$ valid for small $\delta_i = \delta_f \ll 1$. As a result, in the PARA configuration the reversal time increases with increasing strength of the dipolar interaction. The sensitivity of the data to the parameters δ_i (where δ_f is fixed or vice versa) is illustrated in Fig. 2(b): In accordance with Eq. (7), the reversal time depends only logarithmically on the quantity and does not change its order of magnitude while δ_i is changing over several powers of 10. Thus our results are not qualitatively affected by our choice of the condition $\delta_i = \delta_f = 0.001$.

A similar result regarding the sensitivity to initial conditions is obtained in the PERP configuration. Here an analytical result comparable to Eq. (7) does not seem to be

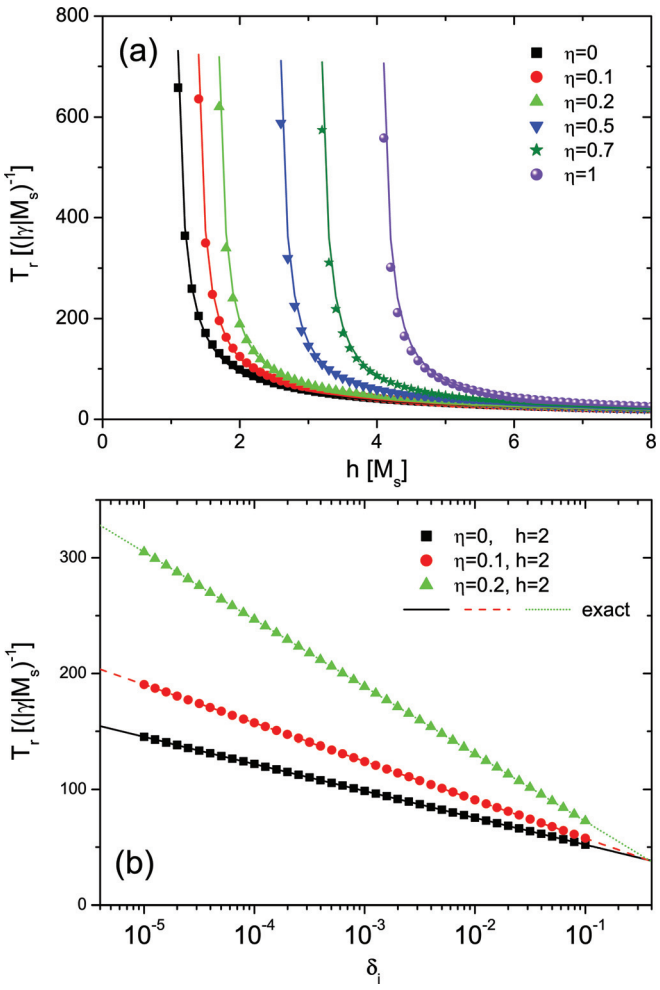

FIG. 2. (Color online) PARA configuration: (a) Reversal time T_r versus field magnitude h at different DDI strength η. The simulation data (symbols) is fitted according to the approximate expression $T_r \simeq [2\lambda h(-\ln\delta_i)]/(h^2 - h_0^2)$ for $\delta_i = \delta_f = 0.001$, and $k = 0.5$, $\alpha = 0.1$ (cf. Fig. 1). (b) Dependence of T_r on the initial condition δ_i: Simulation data along with exact analytical results according to Eq. (7). The final state is fixed to be $\delta_f = 0.001$.

achievable. However, the simulation data is shown in Fig. 3(b) that T_r again depends only logarithmically on δ_i and is therefore similarly insensitive to the initial condition as in the PARA case. The dependence of the reversal time on the dipolar parameter η shown in Fig. 3(a), however, is strikingly different from the PARA configuration: Here T_r clearly decreases with increasing η, especially in the regime of low fields, which also strongly favors the two-body bit implementation proposed in this paper.

C. Zero-field Reversal

From the previous discussion we notice that, around the critical DDI strength η_c, we find not only nearly a zero critical switching field but also a substantially shorter reversal time. This result promises attractive future applications for computer technology, such as fast read/write hard disk or magnetic memory. Let us discuss two schematic setups for experimentally realizing the zero-field switching mechanism. The first scheme A is illustrated in the upper-left panel of Fig. 4, along with a numerical simulation in Fig. 4(a). Here we chose again $k = 0.5$, and the DDI parameter is $\eta = 0.32 < \eta_c = 1/3$. Thus, the magnetization in the zero-field ground state of the synchronization mode points along the EA (z-axis).[31] Implementation steps of scheme A are demonstrated as follows: *Step 1*—First we choose a casual initial condition near this ground state, for instance $m_{1z}(0) = m_{2z}(0) = 0.5$, to mimic the relaxation of the system to the parallel state under zero-field during $0 < t < 500$; *Step 2*—Then we apply a tiny antiparallel field $h = 0.03$ during $500 < t < 1000$ which drives the magnetization reversal process of the two-body Stoner particle along the field direction. The reversal time is found to be $T_r \approx 198(|\gamma|M_s)^{-1}$, and the inset in Fig. 4(a) shows the reversal process on a smaller scale; *Step 3*—Finally we quench the field and obtain the new stable parallel magnetic state along the opposite direction.

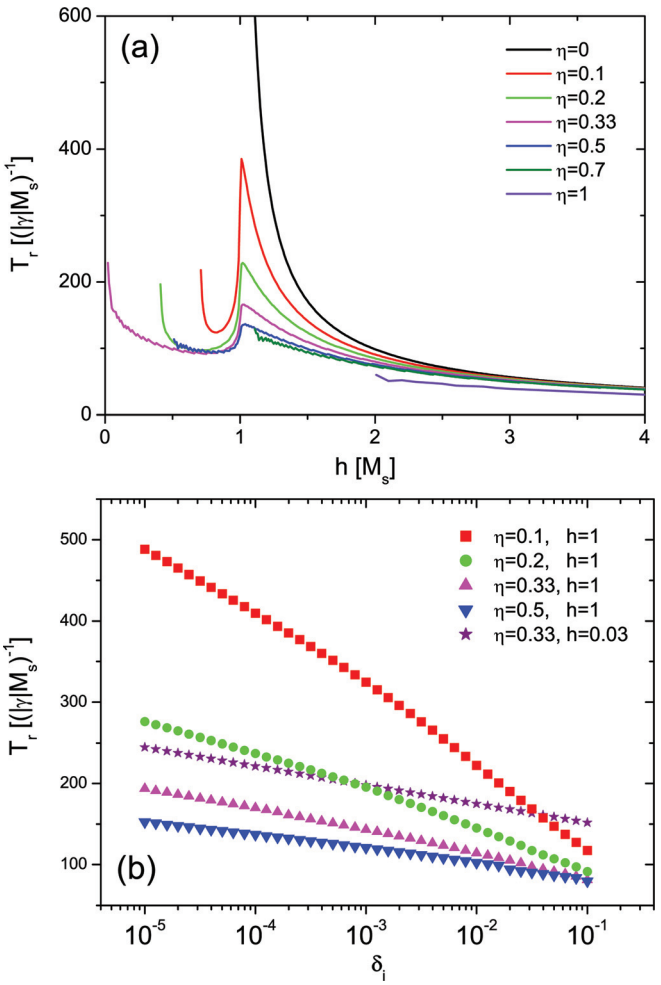

FIG. 3. (Color online) PERP configuration: (a) Reversal time T_r obtained from numerical simulations vs field magnitude h at different DDI strength η. (b) T_r as a function of the initial condition δ_i. All other parameters are the same as Fig. 2.

The second scheme B is sketched in the upper-right panel of Fig. 4 along with a numerical simulation in Fig. 4(b). Here $\eta = 0.34 > \eta_c = 1/3$ for $k = 0.5$, i.e., the zero-field ground state in the synchronization mode is along the hard axis (x-direction), and a field along the EA is permanently required to preserve the magnetization state (information).[32] However, our results show that such a field can be very small and actually close to 0. Thus, it is not implausible to generate such a field as the Oersted field of tiny switchable currents. The reversal process can be implemented as follows: *Step 1*—We again choose the initial condition $m_{1z}(0) = m_{2z}(0) = 0.5$, and the system relaxes to its metastable ground state (x-axis) during $0 < t < 500$. Then we apply a tiny field $h = -0.03$ (note our definition $\vec{h} = -h\hat{z}$) to preserve the magnetic state $m_z = 1$ during $500 < t < 1000$; *Step 2*—After $t > 1000$ the field is reversed to $h = 0.03$, and the two-body particle reverses its magnetization during a reversal time as $T_r \approx 155(|\gamma|M_s)^{-1}$ [see also inset in Fig. 4(b)]; *Step 3*—The reverse field is applied permanently to preserve the reversal bit information.

D. Discussion

We now address the stability of the synchronization dynamics of the two-body particle as studied so far. Let us first investigate small deviations of the initial magnetization directions of the two subparticles being otherwise still identical. In detail, we fixed the initial direction (at $t = 500$ in reversal scheme A, and at $t = 1000$ for scheme B) of one subparticle to be close to the z-axis, i.e., $\theta_1 = 0.001$, and changed the other initial direction to $\theta_2 = 0.001 + \delta$. The result is shown in Fig. 4(c) and 4(e): For a finite range of deviations, $\delta < 7.8°$ ($\delta < 4.5°$) in scheme A(B), the synchronized motion remains stable, while for substantially larger δ, the average magnetization mostly reaches zero.

Let us now consider another case where the two particles differ slightly in anisotropy K_i, volume V_i, saturation magnetization $M_{s,i}$ ($i = 1, 2$). Here the zero-field mechanism still occurs at $\eta_c = (k_1 + k_2)/3 = \frac{2(K_1V_1+K_2V_2)}{3\mu_0 M_{s1}M_{s2}(V_1+V_2)}$. However, the effective field experienced by each particle will also be slightly different. To numerically check the stability under such different external fields, we fixed the field on one subparticle to $h_1 = 0.03$ and changed the field on the other subparticle as $h_2 = 0.03 + \delta h$. The numerical results are given in Fig. 4(d) and 4(f) for reversal schemes A and B, respectively, and demonstrate again a finite range of stability against deviations from the case of strictly identical particles.

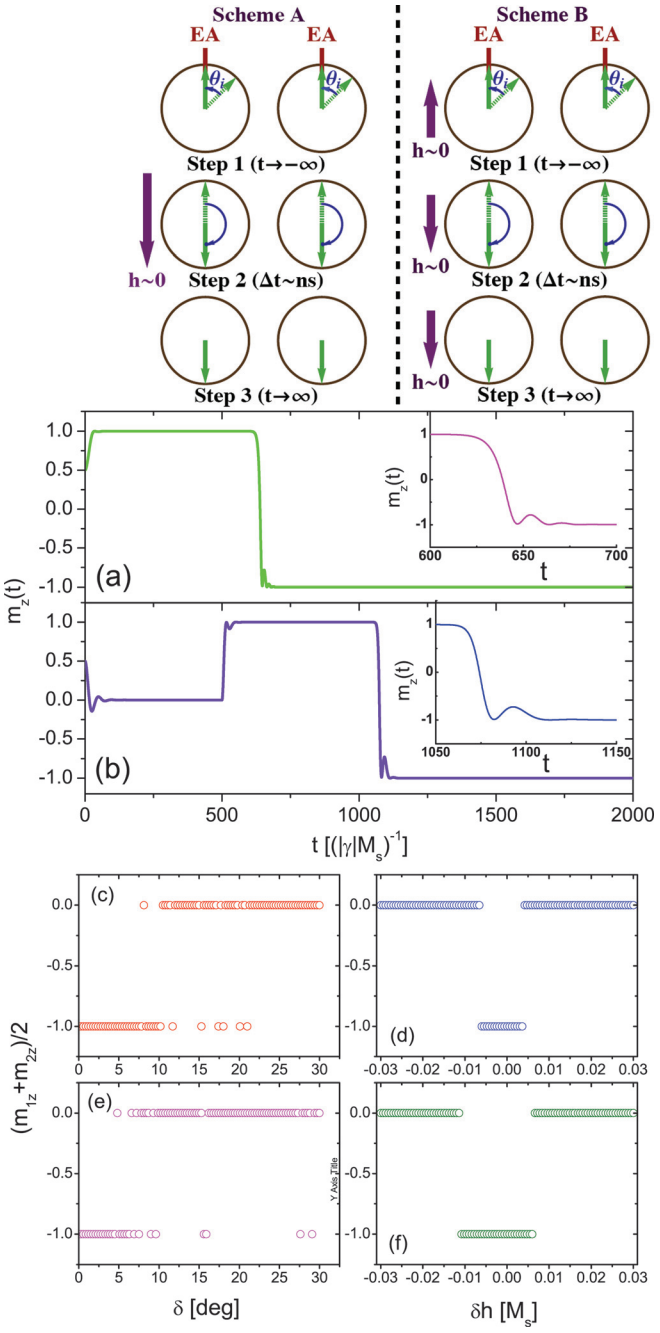

FIG. 4. (Color online) Upper panels: Two schemes of zero-field reversals of the two-body Stoner particle. Scheme A: A magnetic field (h) is applied only during step 2 with nanoseconds; Scheme B: h is always applied with changing its direction from step 2. Middle panels: $m_z(t)$ versus time at (a) $\eta = 0.33 < \eta_c = 1/3$, (b) $\eta = 0.34 > \eta_c = 1/3$. In (a), an antiparallel field $h = 0.03$ is applied only during the time interval $500 < t < 1000$ with a reversal time of $T_r \approx 198(|\gamma|M_s)^{-1}$; In (b), a parallel field $h = -0.03$ is applied during $500 < t < 1000$ and then reversed to $h = 0.03$, leading to a reversal time as $T_r \approx 155(|\gamma|M_s)^{-1}$. The insets show the reversal process on a smaller scale. Bottom panels (c) & (e): Average stable magnetization $(m_{1z} + m_{2z})/2$ vs the deviation angle $\delta = \theta_2 - \theta_1$ (in degrees) between the initial magnetization directions in the two schemes A and B, respectively. The starting width of δ: (c) $0 - 7.8$ and (e) $0 - 4.5$ reveals the stability ranges for the synchronized dynamics. (d) and (f): Analogous data as a function of the deviation field $\delta h = h_2 - h_1$ antiparallel to the easy axis in two schemes. The width of δh: (d) $-0.006 - 0.003$ and (f) $-0.011 - 0.006$ shows the stability ranges.

Numerically we have also checked that a slight deviation in the damping parameter α of the two particles will result in a similar synchronization stability range in both schemes. The dependence of the initial angle deviations [δ in Fig. 4(c) and 4(e)] and the effective field differences [δh in Fig. 4(d) and 4(f)] on the damping parameter α has been also numerically investigated. It is shown that large α will enlarge the stability range for initial angle deviation, however the stability range for δh increases at small damping and decreases for larger α, i.e., an optimal α value exists where a maximum deviation of δh occurs. The details will be presented elsewhere.

To give a concrete and practical example of our findings, let us discuss the case of cobalt (Co) particles. The standard data is $M_s = 1400$ kA/m, uniaxial strength $K = 10^5$ J/m^3, $\alpha = 0.1$.[13] Thus $k = K/(\mu_0 M_s^2) = 0.04$ such that $\eta_c = 0.027$. For two spherical particles with radius r, i.e., the DDI parameter $\eta = r^3/(3d^3)$, the critical DDI strength is reached at $d_c = 2.3r$. The critical switching field without DDI (SW limit) is $H_{SW} = 2K/(\mu_0 M_s) = 1400$ Oe. In the presence of DDI, and considering deviations Δd from d_c, one can express the critical switching field as $H_c/H_{SW} = 3|\Delta d|/d_c$. Thus, in order to drastically reduce the switching field by taking advantage of our proposal, one has to engineer the interparticle distance on a scale of $d_c = 2.3r$ which is typically a few hundred nanometers. In the case of Co, the time unit is $(|\gamma|M_s)^{-1} = 3.23$ ps rendering the reversal times in the schemes A and B to be $T_r \approx 0.64$ ns and $T_r \approx 0.5$ ns, respectively, which are much shorter than in the conventional setup.

Another important issue concerns thermal fluctuations. For $\eta < \eta_c$ the ground state ($\theta = 0, \pi$) in the synchronized motion is stable if the energy barrier in presence of DDI is large compared to the thermal energy $3(\Delta\eta)\mu_0 M_s^2 V \gg k_B T$ (k_B: Boltzmann's constant), which translates for $T = 400$K and the above parameters for Co into $(\Delta\eta)r^3 \gg 0.18\,\text{nm}^3$. On the other hand, the energy scale of the applied field should also be large compared to thermal effects, $2\mu_0 M_s HV \gg k_B T$, which, under the same conditions, reduces to $H \gg 4700/r^3$ Oe nm^3. Thus, considering a typical particle radius of $r = 100$ nm, i.e., $d_c = 230$ nm, and $H_c/H_{SW} = 0.03$, i.e., $H_c = 42$ Oe, both conditions are easily satisfied, $(\Delta\eta)r^3 = 810\,\text{nm}^3 \gg 0.18\,\text{nm}^3$ and $H_c = 42\,\text{Oe} \gg 0.0047$ Oe.

Finally, we would like to remark that our general results regarding the influence of dipolar interaction on the critical switching field of two-body Stoner particles are consistent with recent experimental and micromagnetic simulation results showing that the coercive field for an array of nanowires can be lower than for a single nanowire.[33] The effects due to more complicated dipolar interaction forms of nonspherical particles at close distances and the nonuniform magnetization excitation will be also interesting for the proposed synchronized dynamics, but the detailed studies are beyond this paper and may be a future research direction.

IV. CONCLUSION

In conclusion, we have investigated magnetization reversal of two-body Stoner particles system, which could play

the role of an information bit, under a static magnetic field. In presence of magnetic dipolar interaction, a stable synchronized motion of the two dipoles is found, where the modified Stoner-Wohlfarth limit, namely the critical switching field, is analytically obtained and numerically verified. We propose a new technological perspective: by engineering an appropriate dipolar interaction strength (i.e., the interparticle distance), the critical switching field can be dramatically lowered even including zero in a perpendicular configuration where the easy-axes and the connecting line of two particles are perpendicular. Moreover, the dipolar interaction also contributes to substantially shorten the reversal time around the zero-field regime. This result can offer possibilities to new magnetic information storage devices and/or fast magnetic-response devices.

APPENDIX: DERIVATION OF EQ. (7)

To derive Eq. (7), one can write down the dynamical equation of the θ angle in PARA configuration as

$$\lambda\dot{\theta} = h\sin\theta - h_0\sin 2\theta/2, \tag{A1}$$

where $\lambda = \alpha + \alpha^{-1}$, $h_0 = 2k + 3\eta$, k denotes the uniaxial anisotropy and η the dipolar interaction parameter. The reversal time from the initial angle θ_i to the final destination θ_f can be defined as

$$T_r = \int_{\theta_i}^{\theta_f} d\theta/\dot{\theta} = \lambda\int_{\theta_i}^{\theta_f}[h\sin\theta - h_0\sin 2\theta/2]^{-1}d\theta. \tag{A2}$$

The integral can be calculated analytically,

$$T_r = \frac{\lambda}{2}\left(\frac{1}{h-h_0}\ln\left|\frac{1-\cos\theta_f}{1-\cos\theta_i}\right| - \frac{1}{h+h_0} \times \ln\left|\frac{1+\cos\theta_f}{1+\cos\theta_i}\right| - \frac{2h_0}{h^2-h_0^2}\ln\left|\frac{h-h_0\cos\theta_f}{h-h_0\cos\theta_i}\right|\right). \tag{A3}$$

In order to obtain a finite time, i.e. avoiding the metastable points at $\theta = 0$, π, we can let $\theta_i = \delta_i$ and $\theta_f = \pi - \delta_f$, where δ_i, $\delta_f \ll 1$. By using the approximation $\cos\delta_{i,f} \approx 1 - \delta_{i,f}^2/2$ and substituting them into the above equation, one can directly obtain Eq. (7).

ACKNOWLEDGMENTS

We thank Christian Back for useful discussions. This work has been supported by the Alexander von Humboldt Foundation (ZZS), by DAAD-FUNDAYACUCHO (AL), and by Deutsche Forschungsgemeinschaft via SFB 689.

[1]Spin dynamics in confined magentic structures I&II, edited by B. Hillebrands and K. Ounadjela, (Springer-Verlag, Berlin, 2002 and 2003).
[2]Spin dynamics in confined magentic structures III, edited by B. Hillebrands and A. Thiaville, (Springer-Verlag, Berlin, 2006).
[3]M. Hehn, K. Ounadjela, J.-P. Bucher, F. Rousseaux, D. Decanini, B. Bartenlian, and C. Chappert, Science **272**, 1782 (1996).
[4]C. Stamm, F. Marty, A. Vaterlaus, V. Weich, S. Egger, U. Maier, U. Ramsperger, H. Fuhrmann, and D. Pescia, Science **282**, 449 (1998).
[5]S. Sun, C. B. Murray, D. Weller, L. Folks, A. Moser, Science **287**, 1989 (2000).
[6]D. Zitoun M. Respaud, M.-C. Fromen, M. J. Casanove, P. Lecante, C. Amiens, and B. Chaudret, Phys. Rev. Lett. **89**, 037203 (2002).
[7]E. C. Stoner and E. P. Wohlfarth, Philos. Trans. R. Soc. London, Ser. A **240**, 599 (1948).
[8]L. He, W. D. Doyle, and H. Fujiwara, IEEE Trans. Magn. **30**, 4086 (1994); L. He and W. D. Doyle, J. Appl. Phys. **79**, 6489 (1996).
[9]W. K. Hiebert, A. Stankiewicz, and M. R. Freeman, Phys. Rev. Lett. **79**, 1134 (1997).
[10]T. M. Crawford, T. J. Silva, C. W. Teplin, and C. T. Rogers, Appl. Phys. Lett. **74**, 3386 (1999).
[11]Y. Acremann, C. H. Back, M. Buess, O. Portmann, A. Vaterlaus, D. Pescia, and H. Melchior, Science **290**, 492 (2000); Y. Acremann, C. H. Back, M. Buess, D. Pescia, and V. Pokrovsky, Appl. Phys. Lett. **79**, 2228 (2001).
[12]R. L. Stamps, and B. Hillebrands, Appl. Phys. Lett. **75**, 1143 (1999); M. Bauer, J. Fassbender, B. Hillebrands, and R. L. Stamps, Phys. Rev. B **61**, 3410 (2000).
[13]C. H. Back, D. Weller, J. Heidmann, D. Mauri, D. Guarisco, E. L. Garwin, and H. C. Siegmann, Phys. Rev. Lett. **81**, 3251 (1998); C. H. Back, R. Allenspach, W. Weber, S. S. P. Parkin, D. Weller, E. L. Garwin, and H. C. Siegmann, Science **285**, 864 (1999).
[14]H. W. Schumacher, C. Chappert, P. Crozat, R. C. Sousa, P. P. Freitas, J. Miltat, J. Fassbender, and B. Hillebrands, Phys. Rev. Lett. **90**, 017201 (2003); H. W. Schumacher, C. Chappert, R. C. Sousa, P. P. Freitas, and J. Miltat, Phys. Rev. Lett. **90**, 017204 (2003).
[15]C. Thirion, W. Wernsdorfer and D. Mailly, Nat. Mater. **2**, 524 (2003).
[16]Z. Z. Sun and X. R. Wang, Phys. Rev. B **71**, 174430 (2005); Z. Z. Sun and X. R. Wang, Phys. Rev. B **73**, 092416 (2006); Phys. Rev. B **74**, 132401 (2006).
[17]Z. Z. Sun and X. R. Wang, Phys. Rev. Lett. **97**, 077205 (2006); X. R. Wang, P. Yan, J. Lu and C. He, Europhys. Lett. **84**, 27008 (2008).
[18]M. Tsoi, A. G. M. Jansen, J. Bass, W.-C. Chiang, M. Seck, V. Tsoi, and P. Wyder, Phys. Rev. Lett. **80**, 4281 (1998); J. Z. Sun, J. Magn. Magn. Mater. **202**, 157 (1999); E. B. Myers, D. C. Ralph, J. A. Katine, R. N. Louie, and R. A. Buhrman, Science **285**, 867 (1999); J. A. Katine, F. J. Albert, R. A. Buhrman, E. B. Myers, and D. C. Ralph, Phys. Rev. Lett. **84**, 3149 (2000); S. I. Kiselev, J. C. Sankey, I. N. Krivorotov, N. C. Emley, R. J. Schoelkopf, R. A. Buhrman, and D. C. Ralph, Nature **425**, 380 (2003).
[19]J. Slonczewski, J. Magn. Magn. Mater. **159**, L1 (1996); L. Berger, Phys. Rev. B **54**, 9353 (1996); Y. B. Bazaliy, B. A. Jones and S.-C. Zhang, Phys. Rev. B **57**, R3212 (1998).
[20]A. Brataas, Y. V. Nazarov, and G. E. W. Bauer, Phys. Rev. Lett. **84**, 2481 (2000); X. Wanital, E. B. Myers, P. W. Brouwer, and D. C. Ralph, Phys. Rev. B **62**, 12317 (2000); M. D. Stiles and A. Zangwill, Phys. Rev. B **66**, 014407 (2002).
[21]X. R. Wang and Z. Z. Sun, Phys. Rev. Lett. **98**, 077201 (2007).
[22]H. N. Bertram and J. C. Mallinson, J. Appl. Phys. **40**, 1301 (1969); H. N. Bertram and J. C. Mallinson, J. Appl. Phys. **41**, 1102 (1970).
[23]W. Chen, S. Zhang and H. N. Bertram, J. Appl. Phys. **71**, 5579 (1992).
[24]J. J. Lu, M.-T. Liu, C. C. Kuo and H. L. Huang, J. Appl. Phys. **85**, 5558 (1999); H. L. Huang, J. J. Lu, Appl. Phys. Lett. **75**, 710 (1999).
[25]A. Lyberatos and R. W. Chantrell, J. Appl. Phys. **73**, 6501 (1993).
[26]C. Xu, P. M. Hui, J. H. Zhou, and Z. Y. Li, J. Appl. Phys. **91**, 5957 (2002); L. F. Zhang, C. Xu, P. M. Hui, and Y. Q. Ma, J. Appl. Phys. **97**, 103912 (2005).
[27]H. N. Pham, I. Dumitru, A. Stancu, and L. Spinu, J. Appl. Phys. **97**, 10P106 (2005).
[28]A.-V. Plamada, D. Cimpoesu and A. Stancu, Appl. Phys. Lett. **96**, 122505 (2010).
[29]L. Landau and E. Lifshitz, Phys. Z. Sowjetunion **8**, 153 (1953); T. L. Gilbert, Phys. Rev. **100**, 1243 (1955).
[30]Z. Z. Sun, A. Lopez, and J. Schliemann, arXiv:1005.1828.
[31]The parallel initial state is metastable in the whole phase space including non-synchronition motion states. Thus, low thermal exciation or strong exchange interaction between two particles is required for such a initial state.
[32]One might also consider a reversal process along the hard axis mx = 1 to mx = − 1 by applying a field along x direction. However, numerical simulations show that this synchronized motion becomes unstable for such an initial condition. This is different from the reversal process in scheme B (see text).
[33]K. Nielsch, R. B. Wehrspohn, J. Barthel, J. Kirschner, U. G. Ösele, S. F. Fischer, and H. Kronmüller, Appl. Phys. Lett. **79**, 1360 (2001); R. Hertel, J. Magn. Magn. Mater. **249**, 251 (2002).